Chapter 4

Comprehensive Study of Heat Exchangers with Louvered Fins

Latife Berrin Erbay, Bahadır Doğan and Mehmet Mete Öztürk

Additional information is available at the end of the chapter

http://dx.doi.org/10.5772/66472

Abstract

The purpose of this chapter is to describe the basic physical features and the analysis of the thermal-hydraulic performance of the louver fins. The terminology which is used widely in the field of compact heat exchanger with louvered fin is described. The flow phenomenon affected by the operating conditions and the geometric parameters of the louvered fin is examined using the flow visualization techniques found in the literature. A methodology is given to calculate the heat transfer and the friction factor. Stanton number, Colburn *j*-factor and friction factor are defined as a performance criteria and the variations of these criteria with respect to the Reynolds number and the geometric parameters of the louvered fin. The combinations of these dimensionless number such as area goodness factor (j/f), volume goodness factor ($j/f^{1/3}$) and *JF* number related with the volume goodness factor are discussed in terms of overall performance criteria. Finally, the correlations of the louvered fin heat exchanger and their tabulated data was summarized.

Keywords: plate fin, louver fin, compact heat exchanger

1. Introduction

The plate heat fin exchangers have a widely used application area. They are characterized by having secondary surfaces or fin structures. The function of the secondary (extended) surface is the enhancement of heat transfer performance of the heat exchanger in the allowable range of the pressure drop. The commonly used forms of the extended surface of the plate fin heat exchangers are the triangular or rectangular plain fin, offset strip fin, wavy fin, louvered fin and perforated fin as shown in **Figure 1**.

For extended surface application, fin geometries fall into two categories: continuous and interrupted surfaces. Continuous surfaces achieve heat transfer enhancement through the

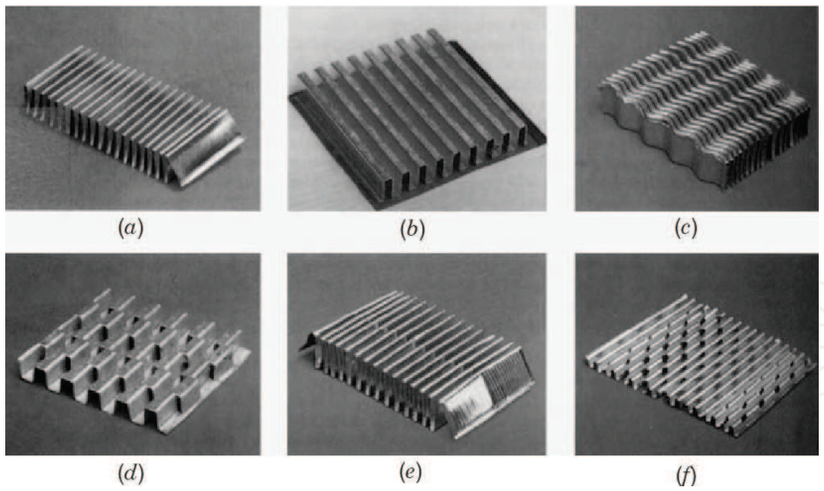

Figure 1. Fin geometries for plate fin heat exchangers: (a) plain triangular fin; (b) plain rectangular fin; (c) wavy fin; (d) offset strip fin; (e) multi-louver fin; (f) perforated fin [1].

secondary flow patterns introduced by sudden velocity changes. On the other hand, interrupted surfaces achieve heat transfer enhancement by the continuous growth and destruction of laminar boundary layers on the interrupted portion of the geometry. One of the mostly used example of the interrupted surface is the louvered fin. The louvered fins were firstly investigated by Kays and London [2] in 1950s, and the popularities of the louvered fins have been maintained.

Today, the use of louvered fins has become popular in the fields of automotive, heating, cooling, air conditioning, power plants and food industry. Typical structure of the louvered fin is shown in **Figure 2**. The efforts of maximize the heat transfer and minimize the pressure drop in heat exchanger design are rapidly increasing due

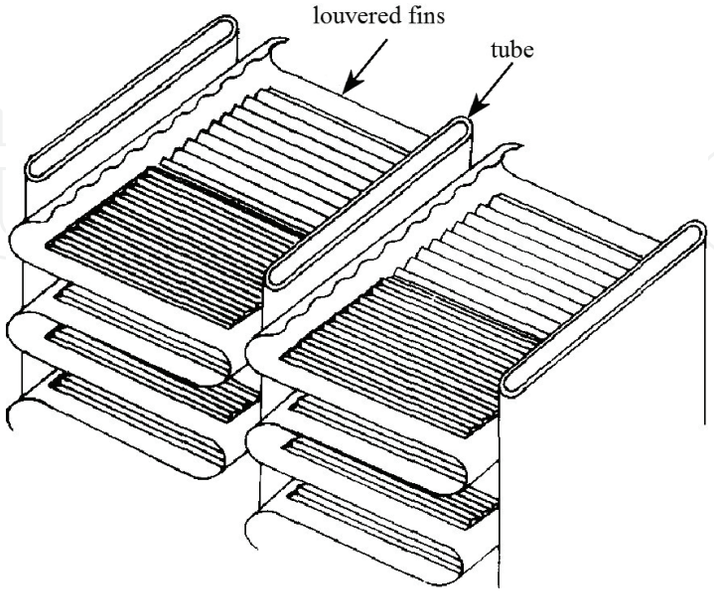

Figure 2. Typical structure of a louver fin geometry [4].

to the restrictions of energy consumption applied by the governments. In this case, the importance of light, high surface density and energy efficient heat exchangers is increasing. The louvered fins are commonly used in heat exchanger field for reasons beyond simply increase the heat transfer surface area and decrease the volume, the amount of coolant and the costs [3].

The louvered fins enhance the heat transfer by providing multiple flat-plate leading edges with their associated high values of heat transfer coefficient. Although the louvered fins are similar in principle to the offset strip fin, they can enhance heat transfer by a factor of 2 or 3 compared with equivalent un-louvered surfaces. The louvers have the further advantage that the enhancement of heat transfer is gained without increase in flow resistance that results from the use of turbulators [5].

Louvers are generally formed by cutting the metal and pushing out the cut elements from the plane of the base metal. They can be manufactured by high-speed production techniques and as a result are less expensive than other interrupted flow geometries when produced in large quantities. Louvered fin geometries can be made in different dimensions of fin length, louver length or material thickness depending on fabrication techniques [2]. The physical principle of the louvered fin is based on the breaking the boundary layer of the flow that passes through the louvers. The structure of the flow phenomenon over the louvered fins is given in details at the following section.

Due to the extensive use of the louvered fins in the heat exchanger area, the researches have spent great efforts to improve the louvered fin geometry from 1950s. In this chapter, first the terminology and the fundamental concepts of flow phenomenon of the louvered fin are explained. In the following sections, the heat transfer and pressure drop characteristics of the louver fins are examined with respect to the geometrical variations of the louvered fin geometry adhering to the experimental and numerical studies in the literature. The empirical correlations are also summarized by a tabulated data.

2. Terminology of the louvered fin

The terminology of a louvered fins was firstly created by Kays and London [2] as shown in **Figure 3**. Each louvered fin configurations is designated by two figures. The first indicates the length of the louvered fin in the flow direction and the second indicates the fin pitch per inch transverse to the flow. Therefore, the meaning of "1/2–6.06" is that each louver has length of 1/2 inch in the flow direction and 6.06 fins in per inch.

Another terminology used for louvered fins with a flat tube is illustrated in **Figure 4**. It is shown from the cross-sectional view that the gap between two louvered fins is called fin pitch (F_p). The length of the flow from the leading edge up to the end of the fin is called flow depth (F_d). The vertical length of the fin and the louver are called fin height and louver height and designated by F_h and L_h, respectively. The horizontal length of the gap between each louver is called louver pitch (L_p), and each louver has an angle of L_α.

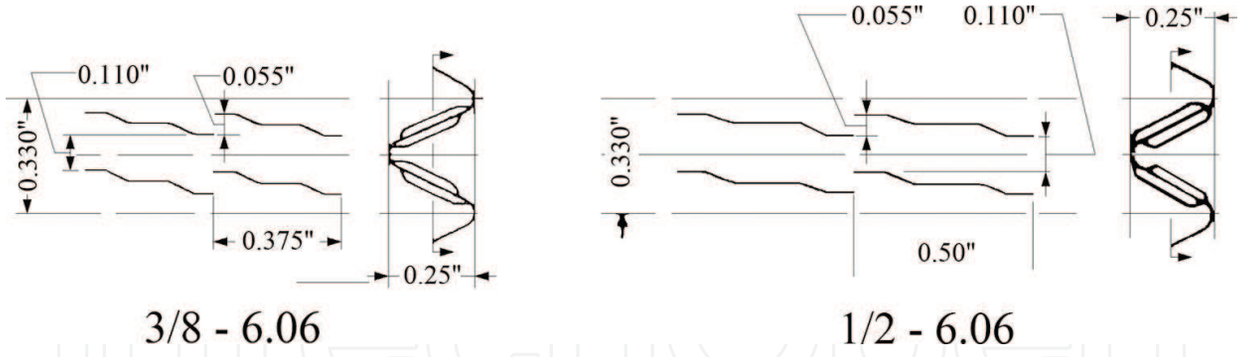

Figure 3. Terminology of the louvered fin [2].

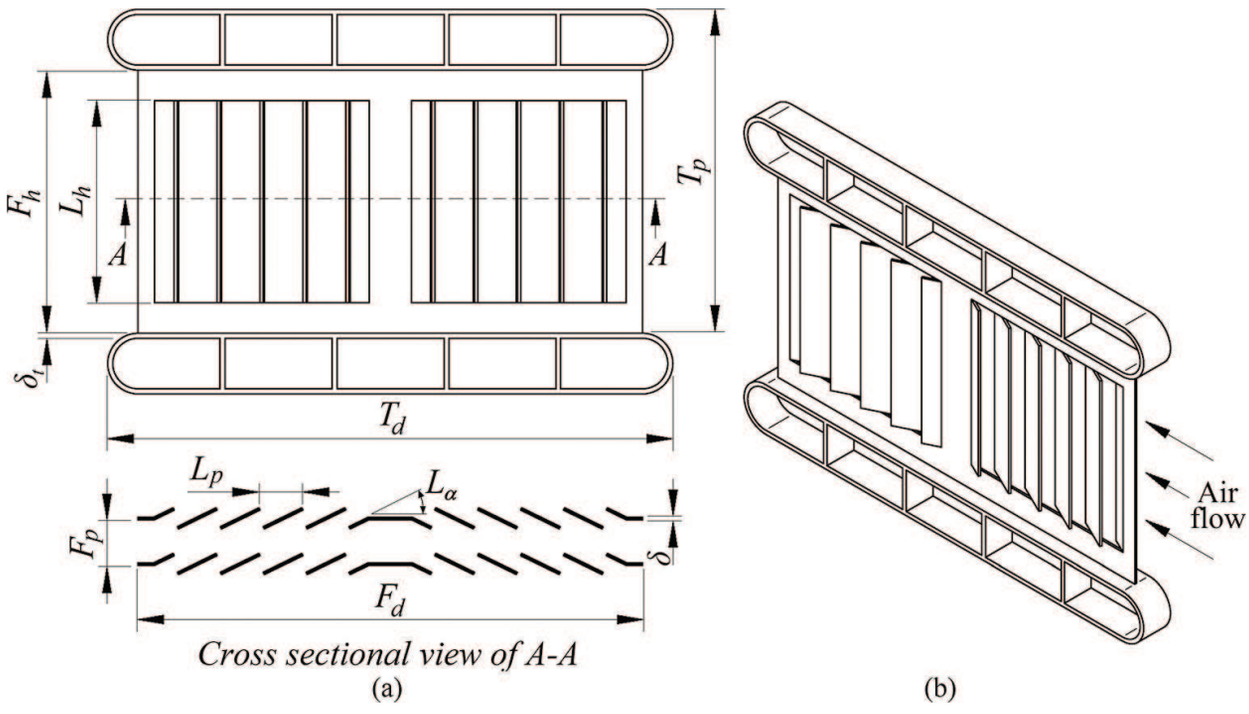

Figure 4. Terminology of the louvered fin [6].

3. Flow phenomenon in louvered fin arrays

The structure of the flow passes through the louvered fins can be identified with flow visualization technique using dye injection and hydrogen bubble. Numerical analysis is also a method to identify the flow phenomenon of louvered fins. Several experimental and numerical studies indicate that the geometric design and the free velocity of the flow effect the direction of the flow through the louvers. As shown in **Figure 5**, the flow enters from the leading edge of the first louver and then directed by the louvers or the fins. If the greatest proportion of the flow is passing between the louvers, it is called "louver directed flow". Similarly, if the greatest proportion of the flow is passing through the gap between the fins, it is called "fin or duct directed flow" [7].

http://dx.doi.org/10.5772/66472

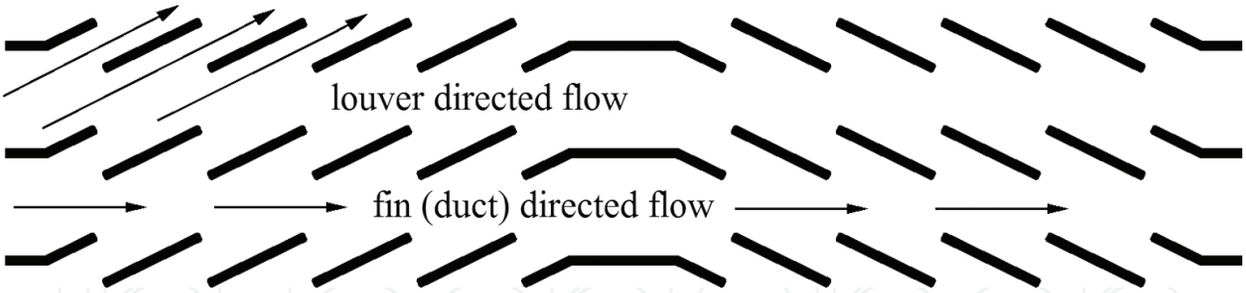

Figure 5. Possible flow direction of flow through the louvered fins.

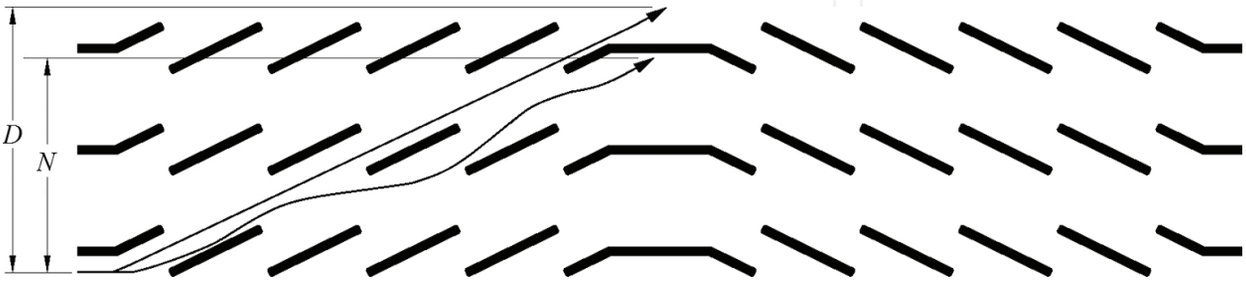

Figure 6. Definition of the flow efficiency.

This definition has revealed another concept called flow efficiency (η) [3]. **Figure 6** provides a visual definition of the flow efficiency, and it is calculated by Eq. (1)

$$\eta = \frac{N}{D} = \frac{Actual\ transverse\ distance}{Ideal\ transverse\ distance} \tag{1}$$

According to the Eq. (1), if the flow efficiency is equal to 1, the flow is parallel to the louvers. If it is equal to zero, the flow is axial through the louvered fin array which is 100% duct flow [3]. **Figure 7** shows the structure of the flow between the louvers. The photographs of the flow through the louvered fin for a louver angle of 26° at a Reynolds number of 500 are obtained using dye injection and hydrogen bubbles techniques. It can be seen that the significant proportion of the flow is directed by the louvers under these circumstances. It is observed that the boundary layers exist on both the upper and lower surfaces of the louver. Flow separation is observed on the back side of the inlet louvers and boundary layer exists on both the upper and lower surfaces of the louvers [3].

Additionally, a large adverse pressure gradient exists on the downstream side of the louvered fin, and the flow separates at the leading edge and forms a large recirculation bubble. **Figure 8a** clearly shows this recirculation zone which is called "first recirculation zone" for a louver angle of 25° at a Reynolds number of 510 using naphthalene sublimation technique by DeJong and Jacobi [8]. This large recirculation zone circulates in a clockwise direction, resulting in a region of very high shear near the trailing edge of the louver where flow that passes downstream between fins interacts with the separation bubble. The high shear results in the formation of a small "secondary recirculation zone" with counter-clockwise rotation in the wake just downstream of the end of the louver. Except at very low Reynolds numbers, a

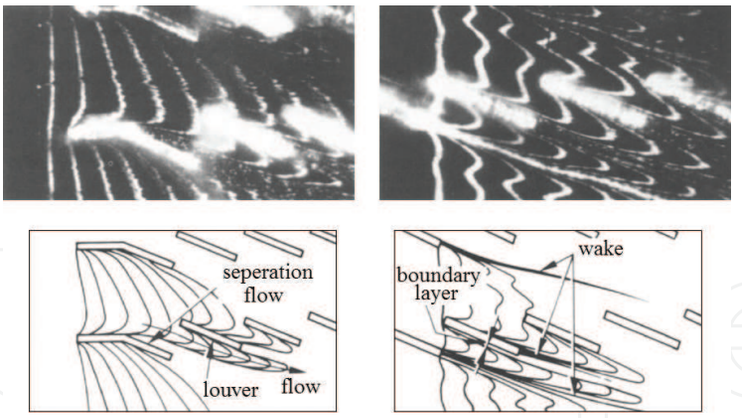

Figure 7. Visualization of the flow in the louvered fin array [3].

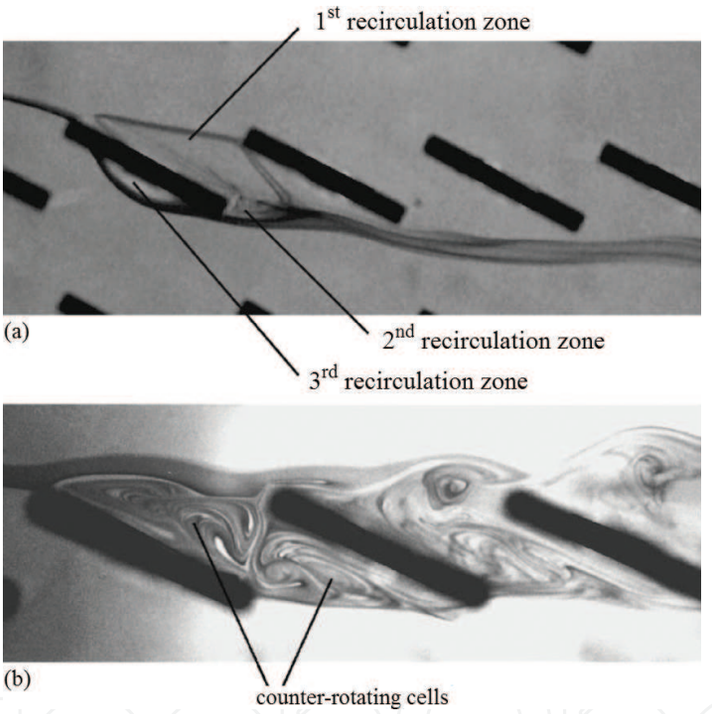

Figure 8. Flow structure around louvered fins: (a) Re = 510, (b) Re = 820 [8].

"third recirculation zone" forms on the upstream side of each louver. This third recirculation zone is caused when the flow passes through the gap between the first recirculation zone and the next louver downstream. This gap is narrow near the leading edge and much larger near the trailing edge. Flow in this gap must decelerate as it passes between the louvers. At all but the lowest Reynolds numbers where the first separation zone is small, the adverse pressure gradient in the inter-louver gap is large enough to cause separation from the upstream face of the next louver. The result is the third recirculation zone with counter-clockwise circulation [8].

Figure 8b shows flow through the same geometry at a higher Reynolds number (820) where the flow has become unsteady. The third recirculation zone has grown to become as large as the first zone, and the small second zone is no longer clearly evident. Two counter-rotating

http://dx.doi.org/10.5772/66472

cells are present between the louvers. Fluid is periodically entrained in the recirculation zones and then ejected in the form of vortices which are carried downstream [8].

Today, the visualization techniques are developing parallel with the rapidly increasing technology. Besides the numerical analysis, infrared technology is a method to identify the flow characteristics of any flow. An open-circuit wind tunnel equipped with an infrared thermo-vision is illustrated in **Figure 9**. Infrared temperature measurement is achieved using an infrared camera. The electromagnetic energy radiated in the infrared spectral band by an object is transformed into an electronic signal by each of the thermo-vision sensors and is obtained simultaneously across the whole field of view, which depend on the optical focal length and the viewing distance [9].

In **Figure 10**, comparison of the experimental results obtained by the infrared measurements and the results of numerical analysis for the same louvered fin geometry is illustrated. The

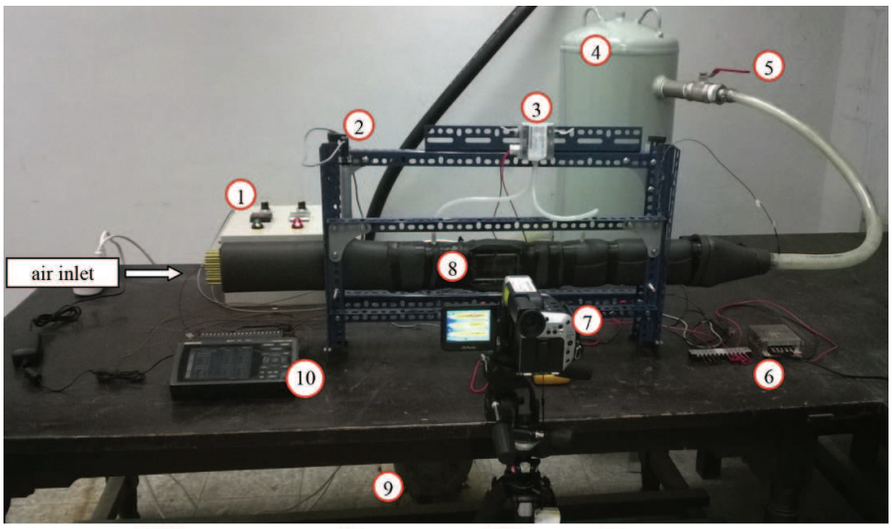

1. Temperature controller
2. Anemometer
3. Pressure gauge
4. Surge tank
5. Flow control valve
6. Power supply
7. Infrared thermal imager
8. Test model
9. Air blower
10. Data acquisition instrument

Figure 9. Wind tunnel test equipped with an infrared thermo-vision [9].

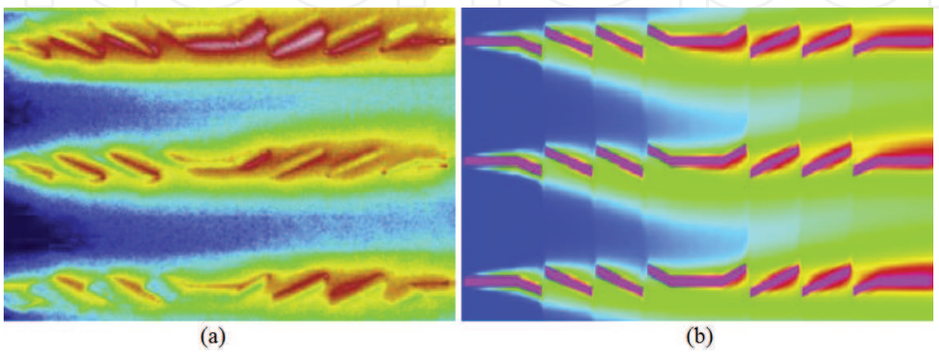

(a) (b)

Figure 10. Comparison of the temperature distribution of an infrared thermographs and numerical simulation results for a louvered fin array [9].

louvered fin has a louver angle of 20° and the flow velocity is 1.0 m/s. It is observed that both methods give similar temperature distributions across the entire louvered fin.

4. Data reduction in a louvered fin heat exchanger

In this section, the calculation method of the performance of a louvered fin heat exchanger is summarized. The equations will be written by considering the following assumptions.

I. Cold flow is the external flow of the louvered fin heat exchanger.

II. Hot flow is the internal flow of the louvered fin heat exchanger.

III. Thermophysical properties of both fluid are constant.

IV. The louvered fins are attached to a mini-channel flat tube.

V. Cold flow is uniform at the inlet of the louvered fin for the numerical analysis.

VI. The temperature of the tube wall is constant for the analytical solutions.

The main problem is the determination of external side heat transfer coefficient for the louvered fin surfaces by experimentally. Effectiveness-*NTU* method is generally used to determine the external side heat transfer coefficient by following the Kim and Bullard [10] method.

The average heat transfer rate can be expressed as

$$\dot{Q} = (\dot{Q}_c + \dot{Q}_h)/2 \tag{2}$$

where $\dot{Q}_c$and $\dot{Q}_h$ are the heat transfer rates of cold and hot fluid, respectively. The heat transfer rates of each fluid can be calculated with Eqs. (3) and (4)

$$\dot{Q}_c = \dot{m}_c c_{p,c}(T_{c,o} - T_{c,i}) \tag{3}$$

$$\dot{Q}_h = \dot{m}_h c_{p,h}(T_{h,i} - T_{h,o}) \tag{4}$$

The effectiveness of the heat exchanger for one row configuration can be calculated using the following equation for both fluid unmixed

$$\varepsilon = 1 - exp\left[\frac{NTU^{0.22}}{C_r}\{\exp(-C_r NTU^{0.78}) - 1\}\right] \tag{5}$$

where

$$\varepsilon = \dot{Q}/\dot{Q}_{max} \tag{6}$$

$$C_r = \frac{(\dot{m}c_p)_{min}}{(\dot{m}c_p)_{max}} \tag{7}$$

We can obtain overall heat transfer coefficient (*UA*) for the heat exchanger as

$$UA = (\dot{m}c_p)_{min} NTU \tag{8}$$

where

$$UA = \dot{Q}/\Delta T_m \tag{9}$$

ΔT_m is the logarithmic mean temperature difference and that is

$$\Delta T_m = \frac{(T_{h,i} - T_{c,o}) - (T_{h,o} - T_{c,i})}{\ln\left((T_{h,i} - T_{c,o})/(T_{h,o} - T_{c,i})\right)} \tag{10}$$

The external (cold) side heat transfer coefficient (h_c) can be obtained from the following equation by experimentally

$$\frac{1}{\eta_c A_c h_c} = \frac{1}{UA} - \frac{\delta_t}{k_t A_t} - \frac{1}{A_i h_i} \tag{11}$$

h_i is the internal side heat transfer coefficient, and it can be obtained using empirical relations for duct flow. The surface effectiveness (η_c) for a dry surface is

$$\eta_c = 1 - \frac{A_f}{A_c}(1 - \eta_f) \tag{12}$$

where η_f is the efficiency of the fin as given in Eq. (13)

$$\eta_f = \frac{\tanh(ml)}{ml} \tag{13}$$

and

$$m = \sqrt{\frac{h_c P_f}{k_f A_{f,c}}} \tag{14}$$

Equation (14) can be expressed more explicitly using the following equation

$$m = \sqrt{\frac{2h_c}{k_f \delta}\left(1 + \frac{\delta}{F_d}\right)} \tag{15}$$

For the calculation of external side heat transfer coefficient (h_c) by analytically, the flow regime is very important to set up the analytical model. Therefore, Reynolds number is the mandatory parameter for the analytical solution. The flow can be assumed to be laminar at Re_{L_p}<1300 for the louvered fin arrays [3]. The characteristics length of louvered fin array is the louver pitch, so that the Reynolds number is calculated based on the louver pitch

$$Re_{L_p} = \frac{u_{max} L_p}{\upsilon} \tag{16}$$

u_{max} is the maximum velocity of the external fluid due to the narrowing section of the louvered fin arrays relatively to the inlet of the louvered fin. Therefore, the free velocity of the external

fluid (u) at the inlet of the louvered fin is transformed to maximum velocity using the following equation

$$u_{max} = uF_p/(F_p - t) \tag{17}$$

where F_p and t are the fin pitch and the material thickness, respectively.

If the tube wall temperature is assumed constant for the numerical analysis, the heat transfer can be calculated by the heat gain of the external (cold) fluid as given in Eq. (3). Thus, the heat transfer coefficient of the external side (h_c) can be obtained from Eq. (18) by numerically

$$h_c = \dot{Q}_c/(A\Delta T_m) \tag{18}$$

In Eq. (18), A is the total external side heat transfer area and ΔT_m is the logarithmic mean temperature difference under constant wall temperature condition given by Eq. (19) [11]

$$\Delta T_m = \frac{(T_w - T_{c,o}) - (T_w - T_{c,i})}{\ln\left((T_w - T_{c,o})/(T_w - T_{c,i})\right)} \tag{19}$$

5. Performance evaluation criteria of the louvered fin heat exchangers

In the heat exchanger literature, some dimensionless parameters are used as a performance criteria. The commonly used thermal performance criteria are Stanton number and Colburn j-factor given as

$$St = \frac{h_c}{\rho u c_p} \tag{20}$$

$$j = StPr^{2/3} \tag{21}$$

respectively. After the calculation of h_c by experimentally or analytically, Stanton number and Colburn j-factor can be obtained to indicate thermal performance of the louvered fin heat exchanger in a dimensionless form as given with Eqs. (20) and (21). Another performance criteria is the friction factor which is the dimensionless form of the pressure drop for the external side of a louvered fin heat exchanger expressed as

$$f = \left(\frac{A_c}{A}\right)\left(\frac{2\Delta P}{\rho u^2}\right) \tag{22}$$

An alternative equation for the friction factor can be used by considering the entrance, exit and acceleration effects

$$f = \left(\frac{A_c}{A}\right)\left(\frac{\rho_m}{\rho_1}\right)\left(\frac{2\rho_1\Delta P}{G_c^2} - (k_c + 1 - \sigma^2) - 2\left(\frac{\rho_1}{\rho_2} - 1\right) + (1 - \sigma^2 - k_e)\frac{\rho_1}{\rho_2}\right) \tag{23}$$

where A_c is the minimum free flow area for the external side, and k_c and k_e are the coefficients of pressure loss at the inlet and the outlet of the heat exchanger. k_c and k_e can be evaluated according to Kays and London [2]. The overall performance of the louvered fin heat

exchangers can be evaluated with another perspective. The ratio of the *j*-factor to the *f*, the ratio of the *j*-factor to the $f^{1/3}$ and *JF* are the overall performance criteria of the louvered fin heat exchangers used in the literature. *j/f* is known as "area goodness factor"[12, 13] and $j/f^{1/3}$ is known as "volume goodness factor"[6, 14, 15]. *JF* number which is related with the volume goodness factor can be obtained by Eq. (24) [16, 17]. These parameters are dimensionless numbers of the larger—the better characteristics. It is expected that these parameters can effectively evaluate the thermal and dynamic performance of a heat exchanger since it includes both the *j*- and the *f*-factor

$$JF = \frac{j/j_R}{(f/f_R)^{1/3}} \tag{24}$$

where j_R and f_R are the reference values of Colburn *j*-factor and friction factor, respectively.

In light of these explanations, thermal and hydraulic characteristics of the heat exchangers with louvered fins are presented using numerical and experimental studies in the literature.

In 1990s, 2D numerical models were preferred rather than 3D models due to the run time and limited computing power. Nevertheless, 3D models are necessary because of the high compatibility with the experimental results. The velocity and the temperature field of a louvered fin heat exchanger for two different Reynolds numbers are presented in **Figure 11** as a result of 2D numerical model.

It is observed that significant proportion of the air flows through the channels between the fins rather than between the louvers, as indicated by the presence of high velocity streaks in the channels at a Reynolds number of 100 (**Figure 11a, b**). The temperature of the air reach the fin temperature before it leaves the fin, therefore, the heat transfer performance of the second half of the fin is poor. In fact, second half of the fin only causes a pressure loss without any heat transfer at low Reynolds numbers. At a higher Reynolds number of 1600 (**Figure 11c, d**), the boundary layer of the louvers are much thinner, and therefore, the air is directed through the louver passages. A temperature difference is maintained between the air and the fin surface and so every part of the louvered fin contributes to the heat transfer. However, the 2D models is enough for the characteristics of the flow over the louvered fins, it is not possible to say same thing for the thermal performance. The comparison of 2D, 3D and the measured thermal and hydraulic performance of a louvered fin heat exchanger are presented in **Figure 12**.

It can be seen that the 2D model yields reasonably accurate predictions of friction factor, but poor predictions of Stanton number. An obvious way to identify the reasons of the error in the heat transfer is to consider the practical features which are missing from the 2-D model. Two important features which are missing are the tube surfaces and the resistance. The tube surfaces would add to the heat transfer area but would not add significantly to the overall heat transfer rate, because of the thick boundary layer growth on the tubes. The fin resistance would lower the temperature across the fin, and thus the heat transfer from the fin. Another reason of the over prediction of the thermal performance of the louvered fin is that the efficiency of the louvered fin cannot be calculated exactly. Generally, the experimental h_c value is obtained using plate fin surface of the fin efficiency even for the louver fin efficiency due to the absence of the base area of the fin in 2D models. In the literature, 2-D models only consider

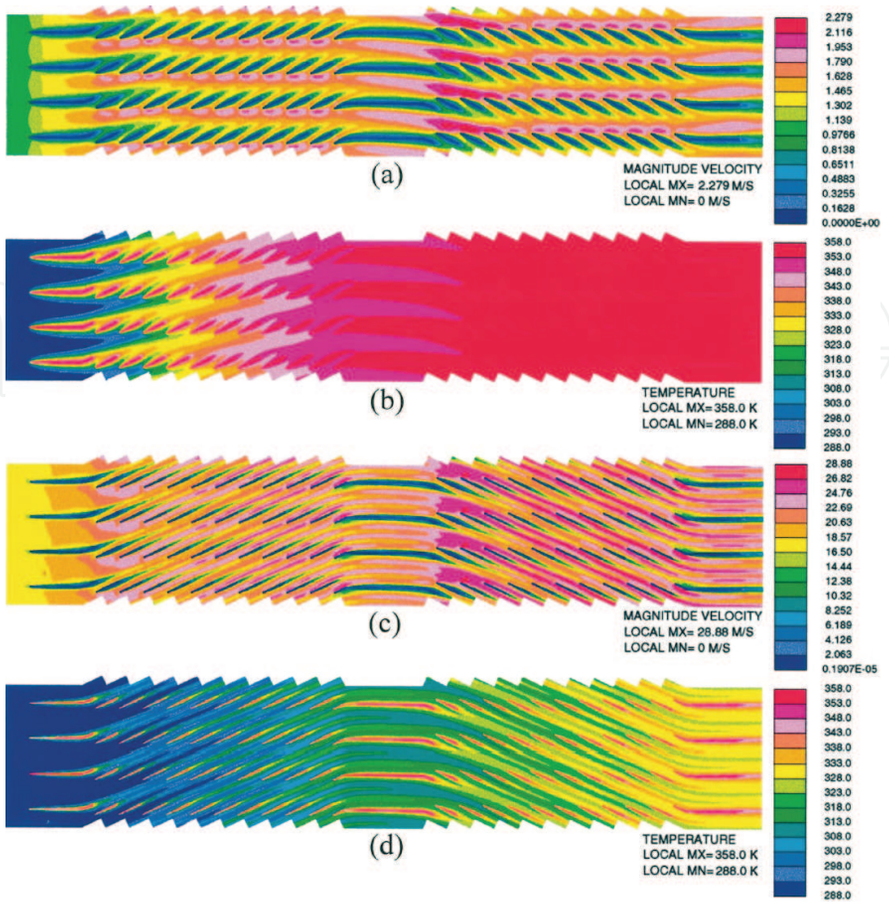

Figure 11. Computed velocity and temperature field for the 2-D model; F_p = 2.54 mm, L_p = 1.4 mm, L_α = 25.5°. (a) Velocity, Re_{Lp} = 100, (b) Temperature, Re_{Lp} = 100, (c) Velocity, Re_{Lp} = 1600, (d) Temperature, Re_{Lp} = 1600 [18].

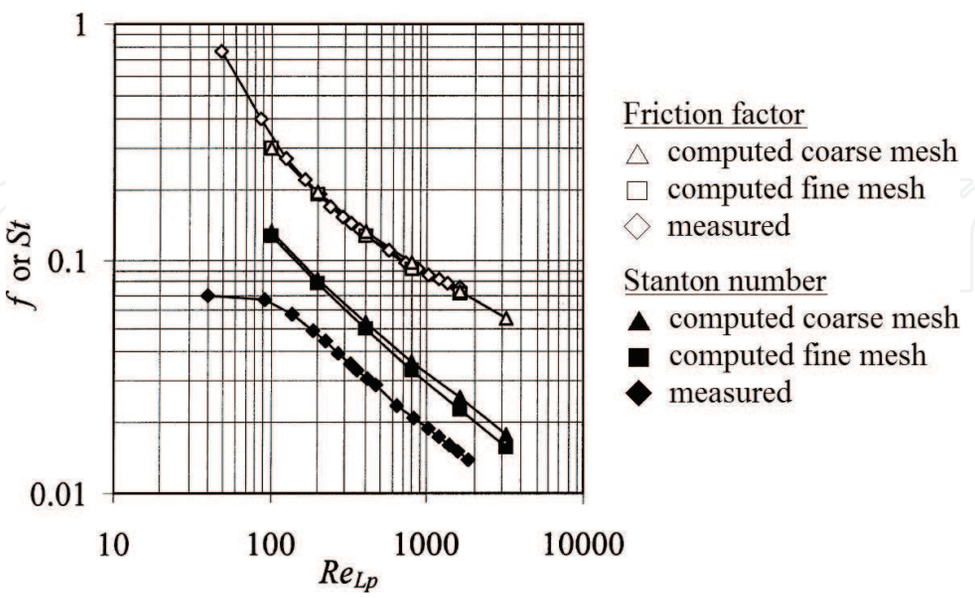

Figure 12. Comparison of the computed 2-D model and measured friction factor and Stanton number: F_p = 2.05 mm, L_p = 1.4 mm, L_α = 25.5°, T_p = 11 mm and δ = 0.05 mm [18].

http://dx.doi.org/10.5772/66472

the cross section of the louvers and the numerical h_c value is used directly without any fin efficiency formula. However, the slopes of the 2D numerical results are comparable and agree with the experimental results, heat transfer coefficient (h_c) is overpredicted with the assumption of constant fin temperature and neglecting the tube surface effect [6, 18, 19]. It is these factors which led to the development of the 3D models.

In 2000s, 3D models have come to the forefront with the increasing computing power. Researchers have begun to compare 2D and 3D results with their own experimental results to validate the compatibility of the numerical models. In **Figures 13** and **14**, the variation of Colburn *j*-factor and the friction factor with respect to the Reynolds number for a louvered fin heat exchanger is presented. The results are also compared with correlations in the literature. It is observed that the CFD results for the 2D models are overpredicted by 80% compared to the experimental results [19]. This is consistent with the study of Atkinson et al. [18]. The slopes of the experimental results are comparable and agree well with the correlated data. Colburn *j*-factor and the friction factor decrease with the increasing of Reynolds number.

Figures 12–14 demonstrate the compatibility of the numerical results with experimental results and the effect of Reynolds number on the thermal and hydraulic performance of the louvered fin heat exchanger. In addition to the effect of Reynolds number, the researchers spent great efforts to determine the optimum geometric parameters of the louvered fin. The numerical studies have a great importance in this field, because the testing of the every geometric variation is very difficult in terms of both time and cost. The prior geometric parameter is the louver angle which has the significant influence on the flow regime over the louvered fins. The variation of the thermal performance of a louvered fin heat exchanger for different louver pitch

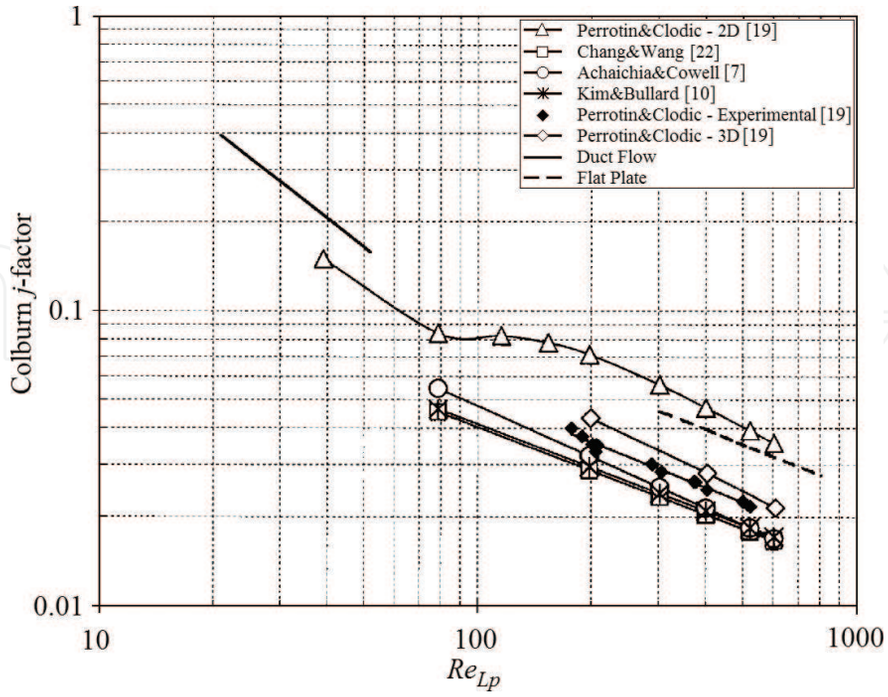

Figure 13. Comparison of computed and measured j-factor [19].

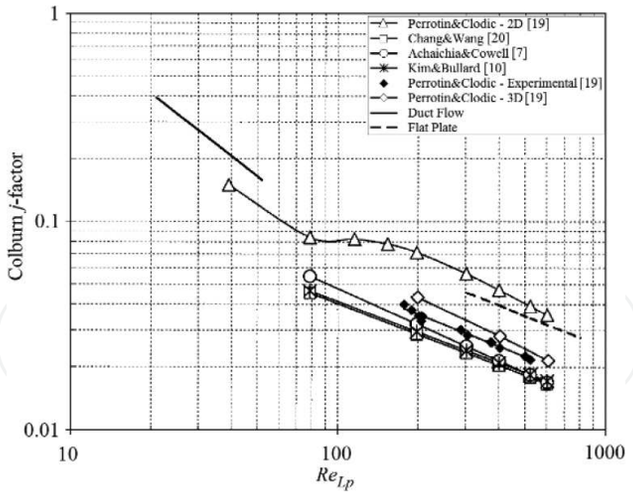

Figure 14. Comparison of computed and measured f-factor [19].

with respect to the louver angle is demonstrated in **Figure 15**. It is observed that the thermal performance is increasing up to the louver angle of 28.5° and then decreasing for all the louver pitches. The louver angle of 28.5° has the maximum thermal performance within the considered cases of the numerical study. Average heat transfer coefficient is about 200 W/m^{2}K at the minimum louver pitch of 0.81 mm. It decreases about to 185 W/m^{2}K at the maximum louver pitch of 1.4 mm [20].

In the study of Atkinson et al. [18], the louvered fin has uniform louver angle. It can be possible to create a louvered fin having non-uniform louver angles as shown in **Figure 16**. **Figure 17** shows the effect of non-uniform louver angle on the thermal and hydraulic performance of a louvered fin heat exchanger.

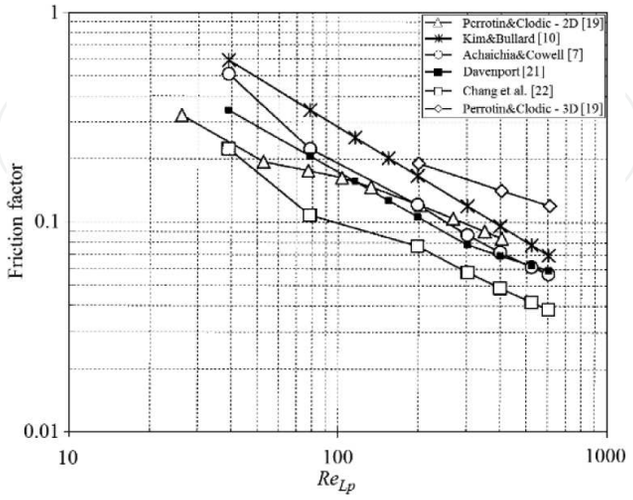

Figure 15. The effect of louver angle on the thermal performance of a louvered fin heat exchanger for different louver pitches [23].

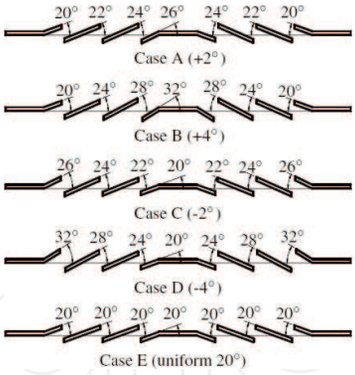

Figure 16. Five different cases of successively increased or decreased louver angle (+2°, +4°, −2°, −4°, and uniform angle 20°) [24].

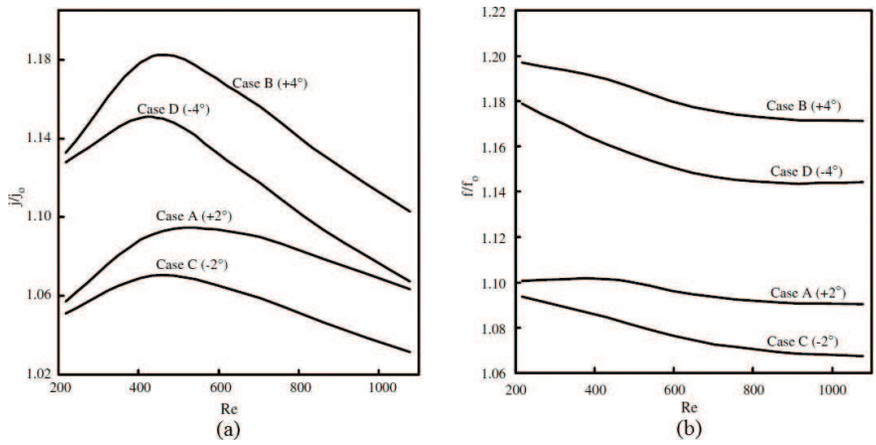

Figure 17. Effect of the non-uniform louver angle on the (a) Colburn j-factor and (b) friction factor [24].

In **Figure 17**, Colburn *j*-factor and the friction factor were normalized with Case E as shown in **Figure 16**. It is seen that the non-uniform louver angle patterns applied in the heat exchangers could effectively enhance the heat transfer performance. Case B has 18% heat transfer enhancement with respect to the Case E about at $Re = 440$. On the other hand, it has a negative effect of %19 on the friction factor.

In most cases, the geometric effects on the performance of a louvered fin heat exchanger are not monotonic. The combined relationship between the louver angle, louver pitch, fin pitch, tube pitch, etc., corrupts the linearity between the geometric parameters and the performance of the heat exchanger. An example is given with **Figure 18**. The variation of the heat transfer coefficient with respect to the frontal air velocity for different tube pitches is illustrated. It is observed that the heat transfer coefficient does not vary with the tube pitch linearly (**Figure 18a**). In **Figure 18b**, the effect of the fin pitch on the heat transfer coefficient is shown. It is seen that the heat transfer coefficient is increasing with decreasing of the fin pitch at a frontal velocity greater than 5.5 m/s. This statement is not valid for the frontal velocity smaller than 5.5 m/s.

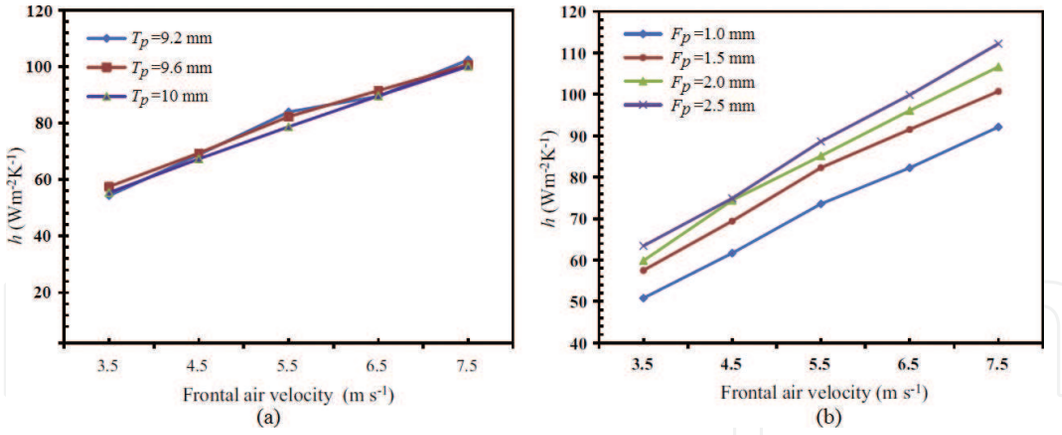

Figure 18. Variation of the heat transfer coefficient with respect to the frontal velocity for different (a) tube pitches (F_p = 1.5 mm, L_p = 1.2 mm, L_α = 26°) and (b) fin pitches (T_p = 9.6 mm, L_p = 1.2 mm, L_α = 26°) [25].

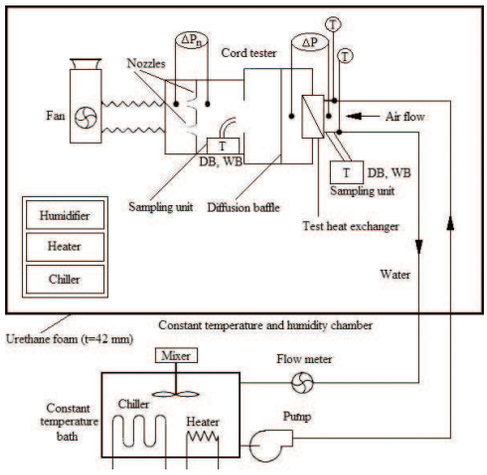

Figure 19. Schematic of a wind tunnel test [10].

Researchers make great efforts to identify the real performances of the louvered fin heat exchangers by experimentally. Investigation of the performance of the louvered fins is commonly performed with the wind tunnel tests. In the open literature, several wind tunnel test can be found in different designs. A typical wind tunnel is shown in **Figure 19**.

As shown in **Figure 19**, internal fluid of the heat exchanger is water and it is regulated by a constant temperature bath. External fluid of the heat exchanger is air, and it is sucked by a fan and wind tunnel is placed in a constant temperature and humidity chamber to regulate the air flow. Dry and wet bulb temperatures of the air are measured with thermocouples at the inlet and the exit of the heat exchanger. One of the most comprehensive performance data of the louvered fin heat exchangers is presented by this wind tunnel test in the early of 2000s. The effects of the geometric dimensions of the louvered fins and the Reynolds number on the Colburn *j*-factor and friction factor is identified. Similarly to the previous studies, *j*-factor and *f*-factor are decreasing with the increasing of Reynolds number due to its definition as shown in **Figure 20**.

http://dx.doi.org/10.5772/66472

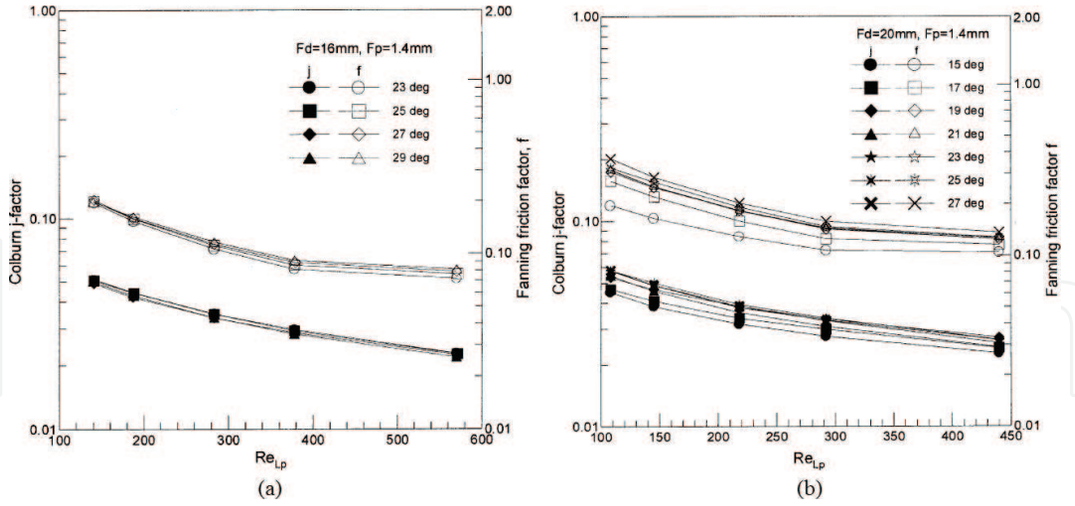

Figure 20. Variations of j-factor and f-factor with respect to the louver angle and Reynolds number for (a) F_d = 16 mm and (b) F_d = 20 mm [10].

The effect of louver angle is more specifically at a flow depth of 20 mm for a constant fin pitch of 1.40 mm. Friction factor increases with the increasing of louver angle, however, the effect of the louver angle is diminishing for the louver angles larger than 21°. The effect of the louver angle on the *j*-factor varies with the flow depth. The increasing in the *j*-factor with the louver angle at a flow depth of 20 mm is more obvious than that of the flow depth of 16 mm. *j*-factor is increasing especially with the louver angle of greater than 23° due to the louver directed flow for such a small fin pitch of 1.40 mm.

The heat transfer and the pressure drop behaviour of the louvered fin heat exchangers for greater flow depths and Reynolds numbers is available in the open literature. The variations of the *j*-factor and *f*-factor with respect to the frontal air velocity for different geometric dimensions are given in **Figure 21**. As shown in **Figure 21**, the considered flow depth and Reynolds number range are 36.0–65.0 mm and 200–2500, respectively.

In **Figure 21a, c**, the effect of fin pitch at a constant flow depth and fin height on the thermal and hydraulic performance is shown. It is observed that the fin pitch has a significant effect on the thermal and hydraulic performance and *j*-factor and *f*-factor are decreasing with the increasing of fin pitch. For F_p = 2.0 mm and F_d = 65 mm, Colburn *j*-factor is maximum for all Reynolds numbers and it decreases about 0.0105–0.0072 as shown in **Figure 21a**. The cause of this situation is that the hydraulic resistance against the flow increases when the fin pitch decreases at the flow passage. Therefore, the flow tends to more to being louver directed. As a result of this phenomenon, the air flow can be mixed well by the louvers, so the heat transfer and the pressure drop increase. As shown in **Figure 21b**, *j*-factor and *f*-factor increase when the fin height increases. The possible reason is that the proportion of the air flow directed by the louvers increases with the fin height. **Figure 21d** shows the effect of the flow depth on the *j*-factor and *f*-factor. It is obvious that the flow depth has more significant effect on the *j*-factor and *f*-factor. The study of Kim and Bullard [10] indicates the same results. In addition to the *j*-factor and *f*-factor, the variation of volume goodness factor denoted by $j/f^{1/3}$ versus Reynolds number is illustrated in **Figure 22** as a performance criteria of the louvered fin heat exchangers.

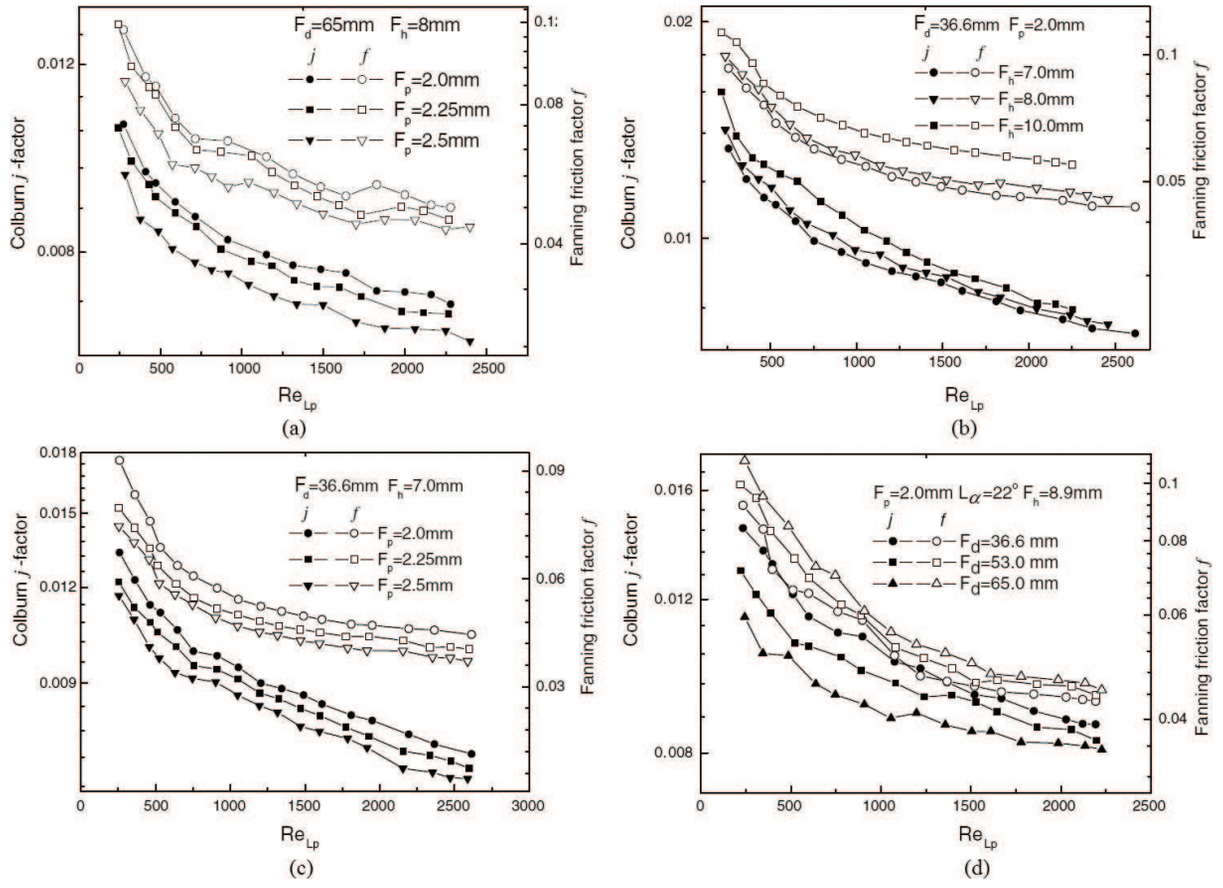

Figure 21. Variations of j-factor and f-factor with respect to the frontal air velocity [15].

It is seen that the geometry which has the smallest flow depth (36.0 mm), smallest fin pitch (2.00 mm) and the biggest fin height (10.0 mm) has the maximum value of $j/f^{1/3}$ = 0.032. The

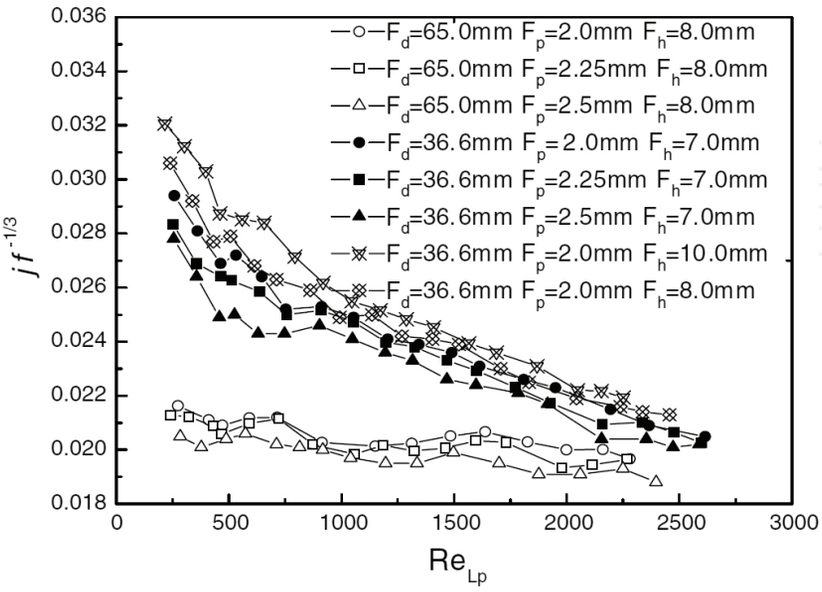

Figure 22. The variation of $j/f^{1/3}$ [15].

http://dx.doi.org/10.5772/66472

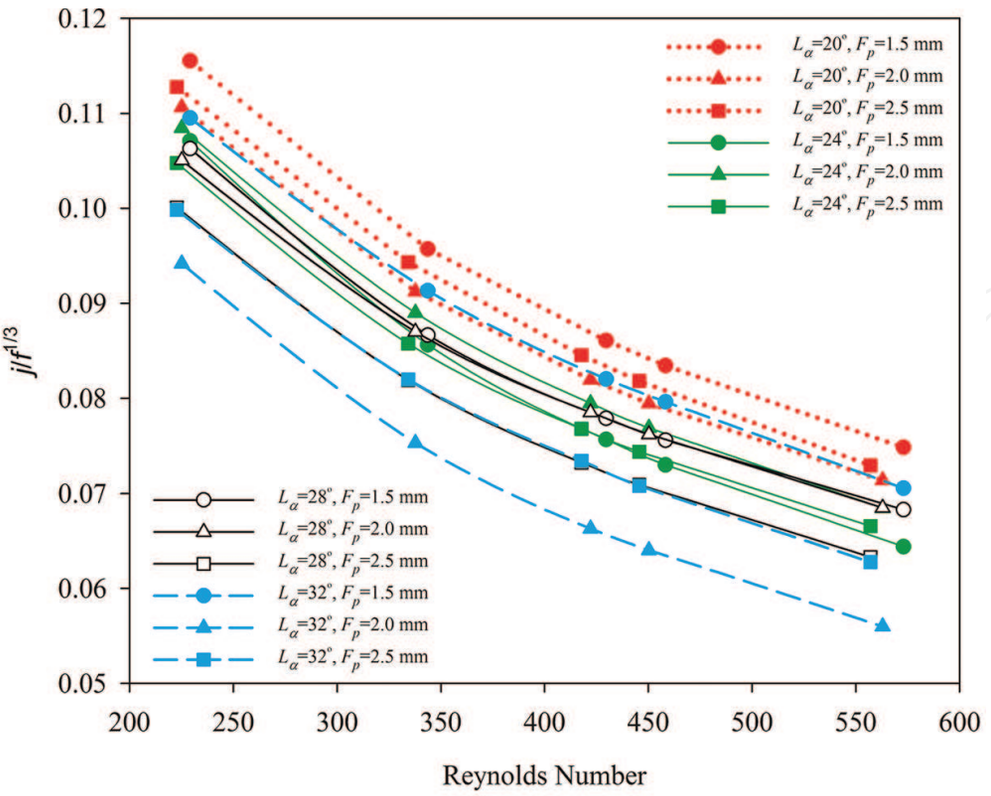

Figure 23. The variation of $j/f^{1/3}$ at low Reynolds number [6].

effect of the Reynolds number to the $j/f^{1/3}$ ratio decreases with a flow depth of 65.0 mm. The most important result is the non-monotonic behaviour of the $j/f^{1/3}$ ratio with the geometric dimensions. The variation of the $j/f^{1/3}$ ratio has a complicated behaviour with respect to the fin pitch and the fin height. In particular, the low Reynolds number region which has the significant changes of $j/f^{1/3}$ ratio for the smaller flow depths can be illuminated with another study by Erbay et al. [6] as shown in **Figure 23**.

The $j/f^{1/3}$ ratios of the study of Erbay et al. [6] are obtained for a constant flow depth of 20 mm by numerically. It seen that the $j/f^{1/3}$ ratio for all the geometries has a similar trend with respect to the Reynolds number; however, there is not linear relationship for the geometric parameters. As a result, such a performance criteria which considers both the thermal and hydraulic performance is necessary to design a heat exchanger.

Some of the researches working on the performance evaluation of the louvered fin heat exchangers have developed correlations for Stanton number, Colburn *j*-factor and friction factor. The basic form of these correlations is

$$a = C_1 Re^{C_2} \tag{25}$$

where a represents the performance criteria, and C_1 and C_2 are dependent on the dimensions of the louvered fin heat exchangers. Some of the correlations for the performance criteria of the louvered fin heat exchangers are listed by considering the studies in the open literature.

- Achaichia and Cowell [7], $150 < Re_{L_p} < 3000$

$$St = 1.54Re_{L_p}^{-0.57}\left(\frac{F_p}{L_p}\right)^{-0.19}\left(\frac{T_p}{L_p}\right)^{-0.11}\left(\frac{L_h}{L_p}\right)^{0.15} \tag{26}$$

$$f = 533.42Re_{L_p}^{0.318(logRe_{L_p}-2.25)}F_p^{-0.22}L_p^{0.25}T_p^{0.26}L_h^{0.33}. \tag{27}$$

- Kim and Bullard [10], $100 < Re_{L_p} < 600$

$$j = Re_{L_p}^{-0.487}\left(\frac{L_\alpha}{90}\right)^{0.257}\left(\frac{F_p}{L_p}\right)^{-0.13}\left(\frac{F_h}{L_p}\right)^{-0.29}\left(\frac{F_d}{L_p}\right)^{-0.235}\left(\frac{L_h}{L_p}\right)^{0.68}\left(\frac{T_p}{L_p}\right)^{-0.279}\left(\frac{\delta}{L_p}\right)^{-0.05} \tag{28}$$

$$f = Re_{L_p}^{-0.781}\left(\frac{L_\alpha}{90}\right)^{0.444}\left(\frac{F_p}{L_p}\right)^{-1.682}\left(\frac{F_h}{L_p}\right)^{-1.22}\left(\frac{F_d}{L_p}\right)^{0.818}\left(\frac{L_h}{L_p}\right)^{1.97}. \tag{29}$$

- Dong et al. [15], $200 < Re_{L_p} < 2500$

$$j = 0.26712Re_{L_p}^{-0.1944}\left(\frac{L_\alpha}{90}\right)^{0.257}\left(\frac{F_p}{L_p}\right)^{-0.5177}\left(\frac{F_h}{L_p}\right)^{-1.9045}\left(\frac{F_d}{L_p}\right)^{-0.2147}\left(\frac{L_h}{L_p}\right)^{1.7159}\left(\frac{\delta}{L_p}\right)^{-0.05} \tag{30}$$

$$f = 0.54486Re_{L_p}^{-0.3068}\left(\frac{L_\alpha}{90}\right)^{0.444}\left(\frac{F_p}{L_p}\right)^{-0.9925}\left(\frac{F_h}{L_p}\right)^{-0.5458}\left(\frac{F_d}{L_p}\right)^{-0.0688}\left(\frac{L_h}{L_p}\right)^{-0.2003} \tag{31}$$

- Ryu and Lee [26], $100 < Re_{L_p} < 3000$

$$j = Re_{L_p}^{(-0.484-1.887/lnRe_{L_p})}\left(\frac{F_d}{L_p}\right)^{0.157}\left(2.24-0.588ln\left(\frac{F_p}{L_p sin L_\alpha}\right)\right) \tag{32}$$

$$f = Re_{L_p}^{-0.433}\left(\frac{F_d}{L_p}\right)^{0.185}\left(1.10 + 4.31\left(\frac{L_\alpha}{90}\right)^2 + 0.836\frac{ln(F_p/L_p)}{(F_p/L_p)^2}\right). \tag{33}$$

In addition to above correlations, a large data bank as shown in **Table 1** was used by Chang and Wang [20], Chang et al. [22], and Park and Jacobi [27] to develop a more sensible correlations for *j*-factor and *f*-factor. These correlations which are the more comprehensive for the louvered fin heat exchangers are listed below.

- Chang and Wang [20], $100 < Re_{L_p} < 3000$

$$j = Re_{L_p}^{-0.49}\left(\frac{L_\alpha}{90}\right)^{0.27}\left(\frac{F_p}{L_p}\right)^{-0.14}\left(\frac{F_h}{L_p}\right)^{-0.29}\left(\frac{T_d}{L_p}\right)^{-0.23}\left(\frac{L_h}{L_p}\right)^{0.68}\left(\frac{T_p}{L_p}\right)^{-0.28}\left(\frac{\delta}{L_p}\right)^{-0.05}. \tag{34}$$

- Chang et al. [22], $100 < Re_{L_p} < 3000$

http://dx.doi.org/10.5772/66472

Source	L_p(mm)	F_p(mm)	F_h(mm)	L_h(mm)	L_α(°)	F_d(mm)	T_d(mm)	T_p(mm)	Δ(mm)	N_{LB}
D(1)[a, b] [21]	3.00	1.55	12.70	9.50	8.4	40.0	40.0	14.00	0.075	2
D(2)[a, b] [21]	3.00	1.55	12.70	9.50	10.4	40.0	40.0	14.00	0.075	2
D(3)[a, b] [21]	3.00	1.60	12.70	9.50	16.7	40.0	40.0	14.00	0.075	2
D(4)[a, b] [21]	2.25	1.55	12.70	9.50	13.4	40.0	40.0	14.00	0.075	2
D(5)[a, b] [21]	2.25	1.56	12.70	9.50	16.0	40.0	40.0	14.00	0.075	2
D(6)[a, b] [21]	2.25	1.56	12.70	9.50	19.2	40.0	40.0	14.00	0.075	2
D(7)[a, b] [21]	1.80	1.55	12.70	9.50	18.8	40.0	40.0	14.00	0.075	2
D(8)[a, b] [21]	1.80	1.59	12.70	9.50	20.8	40.0	40.0	14.00	0.075	2
D(9)[a, b] [21]	1.80	1.58	12.70	9.50	27.8	40.0	40.0	14.00	0.075	2
D(10)[a, b] [21]	1.50	1.53	12.70	9.50	19.6	40.0	40.0	14.00	0.075	2
D(11)[a, b] [21]	1.50	1.59	12.70	9.50	22.8	40.0	40.0	14.00	0.075	2
D(12)[a, b] [21]	1.50	1.60	12.70	9.50	35.9	40.0	40.0	14.00	0.075	2
D(13)[a, b] [21]	1.80	1.63	12.70	9.50	14.2	40.0	40.0	14.00	0.075	2
D(14)[a, b] [21]	3.00	1.56	12.70	9.50	11.2	40.0	40.0	14.00	0.075	2
D(15)[a, b] [21]	2.25	1.68	12.70	11.70	24.1	40.0	40.0	14.00	0.075	2
D(16)[a, b] [21]	2.25	1.65	12.70	11.00	21.4	40.0	40.0	14.00	0.075	2
D(17)[a, b] [21]	2.25	1.65	12.70	10.00	21.4	40.0	40.0	14.00	0.075	2
D(18)[a, b] [21]	2.25	1.63	12.70	9.00	21.4	40.0	40.0	14.00	0.075	2
D(19)[a, b] [21]	2.25	1.60	12.70	8.00	20.3	40.0	40.0	14.00	0.075	2
D(20)[a, b] [21]	3.00	1.54	7.80	7.10	13.9	40.0	40.0	9.18	0.075	2
D(21)[a, b] [21]	2.25	1.53	7.80	7.10	13.8	40.0	40.0	9.17	0.075	2
D(22)[a, b] [21]	1.80	1.54	7.80	7.10	20.4	40.0	40.0	9.18	0.075	2
D(23)[a, b] [21]	1.50	1.55	7.80	7.10	26.1	40.0	40.0	9.19	0.075	2
D(24)[a, b] [21]	2.25	1.49	7.80	7.10	9.5	40.0	40.0	9.14	0.075	2
D(25)[a, b] [21]	2.25	1.51	7.80	7.10	16.5	40.0	40.0	9.16	0.075	2
D(26)[a, b] [21]	2.25	1.51	7.80	7.10	17.7	40.0	40.0	9.16	0.075	2
D(27)[a, b] [21]	2.25	1.23	7.80	7.10	16.0	40.0	40.0	8.93	0.075	2
D(28)[a, b] [21]	2.25	1.01	7.80	7.10	13.9	40.0	40.0	8.74	0.075	2
D(29)[a, b] [21]	2.25	1.54	7.80	7.10	14.2	40.0	40.0	9.18	0.075	2
D(30)[a, b] [21]	2.25	1.51	7.80	6.50	16.6	40.0	40.0	9.16	0.075	2
D(31)[a, b] [21]	2.25	1.54	7.80	6.00	17.6	40.0	40.0	9.18	0.075	2
D(32)[a, b] [21]	2.25	1.50	7.80	5.00	14.4	40.0	40.0	9.15	0.075	2
CW(1)[a, b] [22]	1.32	1.80	16.00	12.44	28.0	22.0	22.0	21.00	0.160	2
CW(2)[a, b] [20]	1.32	2.00	16.00	12.44	28.0	22.0	22.0	21.00	0.160	2
CW(3)[a, b] [20]	1.32	2.20	16.00	12.44	28.0	22.0	22.0	21.00	0.160	2
CW(4)[a, b] [20]	1.42	1.80	19.00	17.18	28.0	22.0	22.0	24.00	0.160	2

Source	L_p(mm)	F_p(mm)	F_h(mm)	L_h(mm)	L_α(°)	F_d(mm)	T_d(mm)	T_p(mm)	Δ(mm)	N_{LB}
CW(5)[a, b] [20]	1.42	2.00	19.00	17.18	28.0	22.0	22.0	24.00	0.160	2
CW(6)[a, b] [20]	1.42	2.20	19.00	17.18	28.0	22.0	22.0	24.00	0.160	2
CW(7)[a, b] [20]	1.48	1.80	16.00	12.78	28.0	26.0	26.0	21.00	0.160	2
CW(8)[a, b] [20]	1.48	2.00	16.00	12.78	28.0	26.0	26.0	21.00	0.160	2
CW(9)[a, b] [20]	1.48	2.20	16.00	12.78	28.0	26.0	26.0	21.00	0.160	2
CW(10)[a, b] [20]	1.53	1.80	19.00	16.07	28.0	26.0	26.0	24.00	0.160	2
CW(11)[a, b] [20]	1.53	2.00	19.00	16.07	28.0	26.0	26.0	24.00	0.160	2
CW(12)[a, b] [20]	1.53	2.20	19.00	16.07	28.0	26.0	26.0	24.00	0.160	2
CW(13)[a, b] [20]	1.69	1.80	16.00	12.15	28.0	32.0	32.0	21.00	0.160	2
CW(14)[a, b] [20]	1.69	2.00	16.00	12.15	28.0	32.0	32.0	21.00	0.160	2
CW(15)[a, b] [20]	1.69	2.20	16.00	12.15	28.0	32.0	32.0	21.00	0.160	2
CW(16)[a, b] [20]	1.55	1.80	19.00	16.17	28.0	32.0	32.0	24.00	0.160	4
CW(17)[a, b] [20]	1.55	2.00	19.00	16.17	28.0	32.0	32.0	24.00	0.160	4
CW(18)[a, b] [20]	1.55	2.20	19.00	16.17	28.0	32.0	32.0	24.00	0.160	4
CW(19)[a, b] [20]	1.86	1.80	19.00	15.25	28.0	38.0	38.0	24.00	0.160	4
CW(20)[a, b] [20]	1.86	2.00	19.00	15.25	28.0	38.0	38.0	24.00	0.160	4
CW(21)[a, b] [20]	1.86	2.20	19.00	15.25	28.0	38.0	38.0	24.00	0.160	4
CW(22)[a, b] [20]	1.59	1.80	16.00	13.18	28.0	44.0	44.0	21.00	0.160	2
CW(23)[a, b] [20]	1.59	2.00	16.00	13.18	28.0	44.0	44.0	21.00	0.160	2
CW(24)[a, b] [20]	1.59	2.20	16.00	13.18	28.0	44.0	44.0	21.00	0.160	2
CW(25)[a, b] [20]	1.53	1.80	19.00	16.84	28.0	44.0	44.0	24.00	0.160	4
CW(26)[a, b] [20]	1.53	2.00	19.00	16.84	28.0	44.0	44.0	24.00	0.160	4
CW(27)[a, b] [20]	1.53	2.20	19.00	16.84	28.0	44.0	44.0	24.00	0.160	4
PSU(1)[a] [20][f]	1.00	1.124	8.00	6.50	30.0	16.0	16.0	9.60	0.157	2
PSU(2)[a] [20][f]	1.016	1.954	9.22	6.858	27.0	20.32	20.32	11.11	0.0508	2
PSU(3)[a] [20][f]	1.016	1.588	9.22	6.858	27.0	20.32	20.32	11.11	0.0508	2
PSU(4)[a] [20][f]	1.016	1.270	9.22	6.858	27.0	20.32	20.32	11.11	0.0508	2
PSU(5)[a] [20][f]	0.94	1.114	9.15	7.62	27.0	16.26	16.26	11.11	0.127	2
AC(1)[a, b] [7]	1.40	2.02	9.00	8.50	25.5	41.6	32.0	11.00	0.05	2
AC(2)[a, b] [7]	1.40	3.25	9.00	8.50	25.5	41.6	32.0	11.00	0.05	2
AC(3)[a, b] [7]	1.40	1.65	9.00	8.50	25.5	41.6	32.0	11.00	0.05	2
AC(4)[a, b] [7]	1.40	2.09	9.00	8.50	21.5	41.6	32.0	11.00	0.05	2
AC(5)[a, b] [7]	1.40	2.03	9.00	8.50	28.5	41.6	32.0	11.00	0.05	2
AC(6)[a, b] [7]	1.40	2.15	9.00	8.50	25.5	20.8	16.0	11.00	0.05	1
AC(7)[a, b] [7]	1.40	1.70	9.00	8.50	25.5	20.8	16.0	11.00	0.05	1
AC(8)[a, b] [7]	0.81	2.11	9.00	8.50	29.0	41.6	32.0	11.00	0.05	2

Source	L_p(mm)	F_p(mm)	F_h(mm)	L_h(mm)	L_α(°)	F_d(mm)	T_d(mm)	T_p(mm)	Δ(mm)	N_{LB}
AC(9)[a, b] [7]	0.81	1.72	9.00	8.50	29.0	41.6	32.0	11.00	0.05	2
AC(10)[a, b] [7]	0.81	3.33	9.00	8.50	29.0	41.6	32.0	11.00	0.05	2
AC(11)[a, b] [7]	1.10	2.18	9.00	8.50	30.0	41.6	32.0	11.00	0.05	2
AC(12)[a, b] [7]	0.81	2.16	9.00	8.50	20.0	41.6	32.0	11.00	0.05	2
AC(13)[a, b] [7]	1.10	2.16	6.00	5.50	28.0	41.6	32.0	8.00	0.05	2
AC(14)[a, b] [7]	1.10	2.17	12.00	11.50	22.0	41.6	32.0	14.00	0.05	2
AC(15)[a, b] [7]	1.10	2.17	9.00	5.50	22.0	41.6	32.0	8.00	0.05	2
WJ(1)[a, b] [28]	1.397	2.117	18.923	16.255	30.0	25.4	25.4	22.99	0.158	2
WJ(2)[a, b] [28]	1.397	1.693	18.923	16.255	30.0	25.4	25.4	22.99	0.158	2
WJ(3)[a, b] [28]	1.397	1.411	18.923	16.255	30.0	25.4	25.4	22.99	0.158	2
WJ(4)[a, b] [28]	1.65	2.117	8.64	7.0987	30.0	25.4	25.4	22.99[c]	0.158	2
WJ(5)[a, b] [28]	1.65	1.693	8.64	7.0987	30.0	25.4	25.4	22.99[c]	0.158	2
WJ(6)[a, b] [28]	1.65	1.411	8.64	7.0987	30.0	25.4	25.4	22.99[c]	0.158	2
R(1)[a, b] [29]	0.85	0.51	2.84	2.13	25.0	15.6	15.6	7.51[c]	0.025	2
SS(1)[a, b] [30]	1.40	1.50	12.5	10.20	22.0	57.4	57.4	14.00[d]	0.06	3
SS(2)[a, b] [30]	1.40	2.00	12.4	10.30	18.5	57.4	57.4	13.90[d]	0.06	2
SS(3)[a, b] [30]	1.30	2.00	12.4	10.00	24.5	37.0	37.0	13.90[d]	0.06	2
SS(4)[a, b] [30]	1.20	1.80	8.6	6.80	24.0	37.0	37.0	10.10[d]	0.04	2
SS(5)[a, b] [30]	1.10	1.80	9.6	6.80	25.5	50.0	50.0	11.10[d]	0.06	2
SS(6)[a, b] [30]	0.50	1.90	8.0	5.00	28.5	47.8	47.8	9.50[d]	0.04	4
T(1)[a] [31]	1.884	1.50	20.0	18.50	35.0	50.0	50.0	25[e]	0.16	2
J(1)[b] [32]	1.40	1.06	7.93	6.93	27.0	15.9	–	9.86	0.102	2
J(2)[b] [32]	1.40	2.12	7.93	6.93	27.0	27.9	–	9.86	0.102	2
J(3)[b] [32]	1.40	1.06	7.93	6.93	27.0	27.9	–	9.86	0.102	2
J(4)[b] [32]	1.14	5.08	12.43	11.15	29.0	25.4	–	14.26	0.114	2
J(5)[b] [32]	1.14	2.12	12.43	11.15	29.0	25.4	–	14.26	0.114	2
J(6)[b] [32]	1.14	1.41	12.43	11.15	29.0	25.4	–	14.26	0.114	2
KB(1)[b] [10]	1.70	1.40	8.15	6.40	15.0	20.0	–	10.15	0.10	2
KB(2)[b] [10]	1.70	1.40	8.15	6.40	17.0	20.0	–	10.15	0.10	2
KB(3)[b] [10]	1.70	1.40	8.15	6.40	19.0	20.0	–	10.15	0.10	2
KB(4)[b] [10]	1.70	1.40	8.15	6.40	21.0	20.0	–	10.15	0.10	2
KB(5)[b] [10]	1.70	1.40	8.15	6.40	23.0	20.0	–	10.15	0.10	2
KB(6)[b] [10]	1.70	1.40	8.15	6.40	25.0	20.0	–	10.15	0.10	2
KB(7)[b] [10]	1.70	1.40	8.15	6.40	27.0	20.0	–	10.15	0.10	2
KB(8)[b] [10]	1.70	1.40	8.15	6.40	23.0	24.0	–	10.15	0.10	2
KB(9)[b] [10]	1.70	1.40	8.15	6.40	25.0	24.0	–	10.15	0.10	2

Source	L_p(mm)	F_p(mm)	F_h(mm)	L_h(mm)	L_α(°)	F_d(mm)	T_d(mm)	T_p(mm)	Δ(mm)	N_{LB}
KB(10)[b] [10]	1.70	1.40	8.15	6.40	27.0	24.0	–	10.15	0.10	2
KB(11)[b] [10]	1.70	1.40	8.15	6.40	29.0	24.0	–	10.15	0.10	2
KB(12)[b] [10]	1.70	1.10	8.15	6.40	23.0	20.0	–	10.15	0.10	2
KB(13)[b] [10]	1.70	1.10	8.15	6.40	23.0	24.0	–	10.15	0.10	2
KB(14)[b] [10]	1.70	1.20	8.15	6.40	23.0	20.0	–	10.15	0.10	2
KB(15)[b] [10]	1.70	1.20	8.15	6.40	23.0	24.0	–	10.15	0.10	2
KYL(1)[b] [14]	2.90	2.82	16.50	12.50	20.0	44.0	–	21.20	0.15	2
KYL(2)[b] [14]	2.90	2.42	16.50	12.50	20.0	44.0	–	21.20	0.15	2
KYL(3)[b] [14]	2.90	2.03	16.50	12.50	20.0	44.0	–	21.20	0.15	2
KYL(4)[b] [14]	2.90	2.82	16.50	12.50	25.0	44.0	–	21.20	0.15	2
KYL(5)[b] [14]	2.90	2.42	16.50	12.50	25.0	44.0	–	21.20	0.15	2
KYL(6)[b] [14]	2.90	2.03	16.50	12.50	25.0	44.0	–	21.20	0.15	2
KYL(7)[b] [14]	2.90	2.82	16.50	12.50	30.0	44.0	–	21.20	0.15	2
KYL(8)[b] [14]	2.90	2.42	16.50	12.50	30.0	44.0	–	21.20	0.15	2
KYL(9)[b] [14]	2.90	2.03	16.50	12.50	30.0	44.0	–	21.20	0.15	2
KYL(10)[b] [14]	2.90	2.82	16.50	12.50	35.0	44.0	–	21.20	0.15	2
KYL(11)[b] [14]	2.90	2.42	16.50	12.50	35.0	44.0	–	21.20	0.15	2
KYL(12)[b] [14]	2.90	2.03	16.50	12.50	35.0	44.0	–	21.20	0.15	2

[a] Correlated data considered by Chang and Wang [20].[b] Correlated data considered by Park and Jacobi [27].[c] Park and Jacobi [27] used half of these pitches because of two fin stocks and a splitter plate between the tubes.[d] Park and Jacobi [27] and Chang and Wang [20] assumed that the tube diameter is 1.50 mm due to the lack of information.[e] Chang and Wang [20] assumed that the tube diameter is 5.00 mm due to the lack of information.[f] Correlated data which was unpublished by R. L. Webb considered by Chang and Wang [20].

Table 1. Geometrical dimensions of the louvered fin heat exchangers in the database [20, 27].

$$f = f_1 f_2 f_3 \tag{35}$$

for Re_{L_p}<150

$$f_1 = 14.39 Re_{L_p}^{\left(-0.805\frac{F_p}{F_h}\right)} \left(log_e\left(1.0 + \left(\frac{F_p}{L_p}\right)\right)\right)^{3.04} \tag{36}$$

$$f_2 = \left(log_e\left(\left(\frac{\delta}{F_p}\right)^{0.48} + 0.9\right)\right)^{-1.435} \left(\frac{D_h}{L_p}\right) (log_e(0.5 Re_{L_p}))^{-3.01} \tag{37}$$

$$f_3 = \left(\frac{F_p}{L_h}\right)^{-0.308}\left(\frac{F_d}{L_h}\right)^{-0.308}\left(e^{-0.1167\frac{T_p}{D_m}}\right)L_\alpha^{0.35} \tag{38}$$

for $150 < Re_{L_p} < 5000$

$$f_1 = 4.97 Re_{L_p}^{0.6049-1.064/L_\alpha^{0.2}}\left(log_e\left(\left(\frac{\delta}{F_p}\right)^{0.5}+0.9\right)\right)^{-0.527} \tag{39}$$

$$f_2 = \left(\left(\frac{D_h}{L_p}\right)log_e(0.3Re_{L_p})\right)^{-2.966}\left(\frac{F_p}{L_h}\right)^{-0.7931\frac{T_p}{T_h}} \tag{40}$$

$$f_3 = \left(\frac{T_p}{D_m}\right)^{-0.0446} log_e\left(1.2+\left(\frac{L_p}{F_p}\right)^{1.4}\right)^{-3.553} L_\alpha^{-0.477}. \tag{41}$$

- Park and Jacobi [27], $27 < Re_{L_p} < 4132$

$$\begin{aligned} j_{cor} = {} & 0.872 j_{Re} j_{low} j_{louver} L_\alpha^{0.219} N_{LB}^{-0.0881}\left(\tfrac{F_h}{L_p}\right)^{0.149}\left(\tfrac{F_d}{F_p}\right)^{-0.259}\left(\tfrac{L_h}{F_h}\right)^{0.54} \\ & \times\left(\tfrac{F_h}{T_p}\right)^{-0.902}\left(1-\tfrac{\delta}{L_p}\right)^{2.62}\left(\tfrac{L_p}{F_p}\right)^{0.301} \end{aligned} \tag{42}$$

where

$$j_{Re} = Re_{L_p}^{[-0.458-0.00874\cosh(F_p/L_p-1)]} \tag{43}$$

$$j_{low} = 1-\sin\left(\frac{L_p}{F_p}L_\alpha\right)\left[\cos h\left(0.049Re_{L_p}-0.142\frac{F_d}{N_{LB}}\right)\right]^{-1} \tag{44}$$

$$j_{louver} = 1-(-0.0065\tan L_\alpha)\left(\frac{F_d}{N_{LB}F_p}\right)\cos\left[2\pi\left(\frac{F_p}{L_p\tan L_\alpha}-1.8\right)\right] \tag{45}$$

$$f_{cor} = 3.69 f_{Re} N_{LB}^{-0.256}\left(\frac{F_p}{L_p}\right)^{0.904}\sin(L_\alpha+0.2)\left(1-\frac{F_h}{T_p}\right)^{0.733}\times\left(\frac{L_h}{F_h}\right)^{0.648}\left(\frac{\delta}{L_p}\right)^{-0.647}\left(\frac{F_h}{F_p}\right)^{0.799} \tag{46}$$

where

$$f_{Re} = \left(Re_{L_p}\frac{F_p}{L_p}\right)^{-0.845}+0.0013Re_{L_p}^{[1.26(\delta/F_p)]} \tag{47}$$

However, the correlations of Stanton number, Colburn *j*-factor and friction factor are defined for a large range of Reynolds number and geometric descriptions for heat exchangers with multi-louvered fins, it is necessary that the performance of every new type of heat exchanger is analysed individually due to the complexity of the combined effects of geometrical and operational parameters [33].

6. Concluding remarks

In this chapter, the structure of the louvered fin is examined in terms of thermal and hydraulic performance by following the studies in the literature. Several experimental and numerical studies are analysed by the authors to present a guide for the louvered fin. It is clear that the geometric parameters such as fin pitch, fin height, louver pitch, louver angle, and flow depth have remarkable effect on the performance of a louvered fin heat exchanger. It can be stated that the combined effects of these parameters must be examined individually to design a high efficiency heat exchanger. The key points of this chapter for the researchers can be summarized as follows:

- Frontal air velocity and the louver angle are the determinative parameters for the flow regime over the louvered fins. The duct directed or louver directed flow can be formed by the effects of these parameters.
- The flow efficiency over the louvered fins is increasing with the louver directed flow.
- 2D numerical models are inadequate to predict the heat transfer coefficient due to the lack of the un-finned areas. 3D numerical is sensible to predict both heat transfer coefficient and friction factor.
- Colburn *j*-factor increases with decreasing fin pitch.
- Friction factor (*f*) decreases with increasing fin pitch.
- The area goodness factor (j/f) and the volume goodness factor ($j/f^{1/3}$) decrease with increasing Reynolds number but they do not have a monotonic relation with the geometric parameters such as fin pitch and louver angle.
- However, the wide range of correlated data is available in the literature, every heat exchanger must be analysed individually due to combined effects of geometric parameters and operating conditions.

Acknowledgements

This research was performed under the Santez Project (00865-STZ.2011–1). The authors would like to thank the Ministry of Science, Industry and Technology and the Research and Development Department of the Arçelik A.Ş. Eskişehir Refrigerator Plant for their support.

http://dx.doi.org/10.5772/66472

Nomenclature

a	Performance criteria
A	Heat transfer area, m^2
A_c	Heat transfer area of the cold side, m^2
$A_{c,f}$	Cross-sectional area of the fin, m^2
A_f	Frontal area, m^2
A_i	Heat transfer area of the hot (internal) side, m^2
A_t	Heat transfer area of the tube, m^2
$c_{p,c}$	Specific heat of the cold fluid, kJ/(kg°C)
$c_{p,h}$	Specific heat of the hot fluid, kJ/(kg°C)
C_r	Heat capacity ratio
D	Ideal transverse distance, mm
D_h	Hydraulic diameter, mm
D_m	Major tube diameter, mm
f	Fanning friction factor
f_{cor}	Fanning friction factor correlation
F_d	Flow depth, mm
F_h	Fin height, mm
F_p	Fin pitch, mm
f_R	Reference value of the friction factor
f_{Re}	Correlation factor for Reynolds number effect
G_c	Air mass flux at minimum cross-sectional area, kg/(m^2s)
h	Heat transfer coefficient, W/(m^2°C)
h_c	Heat transfer coefficient of the cold (external) fluid, W/(m^2°C)
h_i	Heat transfer coefficient of the hot (internal) fluid, W/(m^2°C)
j	Colburn j-factor
j_{cor}	Colburn j-factor correlation
j_{louver}	Correlation factor for louver geometry effect
j_{low}	Correlation factor for low Reynolds number effect
j_R	Reference value of the Colburn j-factor
JF	Performance evaluation criteria related with volume goodness factor
k_c	Pressure loss coefficient at the inlet of the heat exchanger
k_e	Pressure loss coefficient at the exit of the heat exchanger
k_f	Thermal conductivity of the fin material, W/(m°C)
k_t	Thermal conductivity of the tube material, W/(m°C)
l	Half of the fin height (F_h), mm
L_α	Louver angle, degree
L_h	Louver height, mm
L_p	Louver pitch, mm
m	Parameter for the calculation of η_f related with h_c, $A_{c,f}$, P_f and k_f, m^{-1}
$\dot{m}_c$	Mass flow rate of the cold fluid, kg/s

$\dot{m}_h$ Mass flow rate of the hot fluid, kg/s
N Actual transverse distance, mm
NTU Number of transfer unit
P Pressure, Pa
P_f Perimeter of the fin, m
Pr Prandtl number
$\dot{Q}$ Average heat transfer rate, W
$\dot{Q}_c$ Heat transfer rate of the cold fluid, W
$\dot{Q}_h$ Heat transfer rate of the hot fluid, W
$\dot{Q}_{max}$ Maximum heat transfer rate, W
Re Reynolds number
Re_{L_p} Reynolds number based on the louver pitch
T Temperature, °C
$T_{c,i}$ Inlet temperature of the cold fluid, °C
$T_{c,o}$ Outlet temperature of the cold fluid, °C
T_h Parameter with the tube pitch and the major tube diameter: T_p–D_m, mm
$T_{h,i}$ Inlet temperature of the hot fluid, °C
$T_{h,o}$ Outlet temperature of the hot fluid, °C
T_p Tube pitch, mm
T_w Wall temperature, °C
ΔT_m Logarithmic mean temperature difference, °C
St Stanton number
u Free velocity of the external fluid, m/s
u_{max} Maximum velocity of the external fluid, m/s
U Overall heat transfer coefficient, W/(m^2°C)
UA Overall thermal conductance, W/°C

Greek letters

δ Thickness of the fin material, mm
δ_t Thickness of the flat tube material, mm
ε Effectiveness
η Flow efficiency
η_c Surface effectiveness of the cold side
η_f Fin efficiency
υ Kinematic viscosity, m^2/s
ρ Density, kg/m^3

Subscripts

1 Inlet
2 Outlet
m Mean

Author details

Latife Berrin Erbay[1]*, Bahadır Doğan[1] and Mehmet Mete Öztürk[2]

*Address all correspondence to: lberbay@ogu.edu.tr

1 Department of Mechanical Engineering, Faculty of Engineering and Architecture, Eskişehir Osmangazi University, Eskişehir, Turkey

2 Department of Motor Vehicles and Transportation Technology, Vocational School of Transportation, Anadolu University, Eskişehir, Turkey

References

[1] Shah R K, Sekulic D P. Fundamental of Heat Exchanger Design. 1st ed. New Jersey: John Wiley & Sons, Inc.; 2003. 941 p.

[2] Kays W M, London A L. Compact Heat Exchangers. 3rd ed. New York: McGraw-Hill; 1984. 335 p.

[3] Webb R L, Trauger P. How structure in the louvered fin heat exchanger geometry. Experimental Thermal and Fluid Science. 1991;**4**(2):205–217. DOI: 10.1016/0894-1777(91)90065-Y

[4] Aoki H, Shinagawa T, Suga K. An experimental study of the local heat transfer characteristics in automotive louvered fins. Experimental Thermal and Fluid Science. 1989;2(3):293–300. DOI: 10.1016/0894-1777(89)90018-6

[5] Cowell T A, Heikal M R, Achaichia A. Flow and heat transfer in compact louvered fin surfaces. Experimental Thermal and Fluid Science. 1995;**10**(2):192–199. DOI: 10.1016/0894-1777(94)00093-N

[6] Erbay L B, Uğurlubilek N, Altun Ö, Dogan B. Numerical investigation of the air-side thermal hydraulic performance of a louvered-fin and flat-tube heat exchanger at low Reynolds numbers. Heat Transfer Engineering. 2017;**38**(5). DOI: 10.1080/01457632.2016.1200382

[7] Achaichia A, Cowell T A. Heat transfer and pressure drop characteristics of flat tube and louvered plate fin surfaces. Experimental Thermal and Fluid Science. 1988;**1**(2):147–157. DOI: 10.1016/0894-1777(88)90032-5

[8] DeJong N C, Jacobi A M. Flow, heat transfer, and pressure drop in the near-wall region of louvered-fin arrays. Experimental Thermal and Fluid Science. 2003;**27**(3):237–250. DOI: 10.1016/S0894-1777(02)00224-8

[9] Jang J-Y, Chen C-C. Optimization of louvered-fin heat exchanger with variable louver angles. Applied Thermal Engineering. 2015;**91**:138–150. DOI: 10.1016/j.applthermaleng.2015.08.009

[10] Kim M-H, Bullard C W. Air-side thermal hydraulic performance of multi-louvered fin aluminium heat exchangers. International Journal of Refrigeration. 2002;**25**(3):390–400. DOI: 10.1016/S0140-7007(01)00025-1

[11] Xiaoping T, Huahe L, Xaingfei T. CFD simulation and experimental study on airside performance for MCHX. In: International Refrigeration and Air Conditioning Conference; 12–15 July 2010; Purdue University, School of Mechanical Engineering; 2010. p. 1–8.

[12] Joardar A, Jacobi A M. Impact of leading edge delta-wing vortex generators on the thermal performance of a flat tube, louvered-fin compact heat exchanger. International Journal of Heat and Mass Transfer. 2005;**48**(8):1480–1493. DOI: 10.1016/j.ijheatmasstransfer.2004.10.018

[13] Han H, He Y-L, Li Y-S, Wang Y, Wu M. A numerical study on compact enhanced fin-and-tube heat exchangers exchangers with oval and circular tube configurations. International Journal of Heat and Mass Transfer. 2013;**65**:686–695. DOI: 10.1016/j.ijheatmasstransfer.2013.06.049

[14] Kim J H, Yun J H, Lee C S. Heat-transfer and friction characteristics for the louver-fin heat exchanger. Journal of Thermophysics and Heat Transfer. 2004;**18**(1):58–64. DOI: 10.2514/1.9123

[15] Dong J, Chen J, Chen Z, Zhang W, Zhou Y. Heat transfer and pressure drop correlations for the multi-louvered fin compact heat exchangers. Energy Conversion and Management. 2007;**48**(5):1506–1515. DOI: 10.1016/j.enconman.2006.11.023

[16] Yun J-Y, Lee K-S. Influence of design parameters on the heat transfer and flow friction characteristics of the heat exchanger with slit fins. International Journal of Heat and Mass Transfer. 2000;**43**(14):2529–2539. DOI: 10.1016/S0017-9310(99)00342–7

[17] Qi Z-G, Chen J-P, Chen Z-J. Parametric study on the performance of a heat exchanger with corrugated louvered fins. Applied Thermal Engineering. 2007;**27**(2–3):539–544. DOI: 10.1016/j.applthermaleng.2006.06.015

[18] Atkinson K N, Drakulic R, Heikal M R, Cowell T A. Two- and three-dimensional numerical models of flow and heat transfer over louvred fin arrays in compact heat exchangers. International Journal of Heat and Mass Transfer. 1998;**41**(24):4063–4080. DOI: 10.1016/S0017-9310(98)00165-3

[19] Perrotin T, Clodic D. Thermal-hydraulic CFD study in louvered fin-and-flat-tube heat exchangers. International Journal of Refrigeration. 2004;**27**(4):422–432. DOI: 10.1016/j.ijrefrig.2003.11.005

[20] Malapure V P, Mitra S K, Bhattacharya A. Numerical investigation of fluid flow and heat transfer over louvered fins in compact heat exchanger. International Journal of Thermal Sciences. 2007;**46**(2):199–211. DOI: 10.1016/j.ijthermalsci.2006.04.010

[21] Hsieh C-T, Jang J-Y. 3-D thermal-hydraulic analysis for louver fin heat exchangers with variable louver angle. Applied Thermal Engineering. 2006;**26**(14–15):1629–1639. DOI: 10.1016/j.applthermaleng.2005.11.019

[22] Chang Y-J, Wang C-C. A generalized heat transfer correlation for Iouver fin geometry. International Journal of Heat and Mass Transfer. 1997;**40**(3):533–544. DOI: 10.1016/0017-9310(96)00116–0

[23] Davenport C J. Correlations for heat transfer and flow friction characteristics of louvered fin. In: 21st National Heat Transfer Conference; Seattle, New York, USA: AIChE; 1983. p. 19–27.

[24] Chang Y-J, Hsu K-C, Lin Y-T, Wang C-C. A generalized friction correlation for louver fin geometry. International Journal of Heat and Mass Transfer. 2000;**43**(12):2237–2243. DOI: 10.1016/S0017-9310(99)00289-6

[25] Karthik P, Kumaresan V, Velraj R. Experimental and parametric studies of a louvered fin and flat tube compact heat exchanger using computational fluid dynamics. Alexandria Engineering Journal. 2015;**54**(4):905–915. DOI: 10.1016/j.aej.2015.08.003

[26] Ryu K, Lee K-S. Generalized heat-transfer and fluid-flow correlations for corrugated louvered fins. International Journal of Heat and Mass Transfer. 2015;**83**:604–612. DOI: 10.1016/j.ijheatmasstransfer.2014.12.044

[27] Park Y-G, Jacobi A M. Air-side heat transfer and friction correlations for flat-tube louver-fin heat exchangers. Journal of Heat Transfer. 2009;**131**(6):021801–1-11. DOI: 10.1115/1.3000609

[28] Webb R L, Jung S H. Air-side performance of enhanced brazed aluminium heat exchangers. ASHRAE Transactions. 1992;**98**(2):391–401.

[29] Rugh J P, Pearson J T, Ramadhyani S. A study of a very compact heat exchanger used for passenger compartment heating in automobiles, in compact heat exchangers for power and process industries. In: ASME Symposium Series, HTD-Vol. 201; New York: ASME; 1992. p. 15–24.

[30] Sunden B, Svantesson J. Correlation of j- and f-factors for multilouvered heat transfer surfaces. In: 3rd UK National Heat Transfer Conference; London: South Kensington Campus; 1992. p. 805–811.

[31] Tanaka T, Itoh M, Kudoh M, Tomita A. Improvement of compact heat exchangers with inclined louvered fins. Bulletin of JSME. 1984;**27**(224):219–226. DOI: 10.1299/jsme1958.27.219

[32] Jacobi A M, Park Y-G, Zhong Y, Michna G, Xia Y. High performance heat exchangers for air-conditioning and refrigeration applications (non-circular tubes). University of Illinois, Phase II-Final Report. 2005;ARTI-21CR/611–20021

[33] Dogan B, Altun Ö, Ugurlubilek N, Erbay L B. An experimental comparison of two multi-louvered fin heat exchangers with different numbers of fin rows. Applied Thermal Engineering. 2015;**91**:270–278. DOI: 10.1016/j.applthermaleng.2015.07.059

IntechOpen